

# Numerical modeling and development of the prototype of the Bragg peak position detector working in real time mode for hadron therapy facilities

A.A. Pryanichnikov<sup>1</sup>, M.A. Belikhin<sup>1</sup>, A.S. Simakov<sup>1</sup>  
E.V. Altukhova<sup>2</sup>, I.I. Degtyarev<sup>2</sup>, F.N. Novoskoltsev<sup>2</sup>, Yu. V. Altukhov<sup>2</sup>, R. Yu. Sinyukov<sup>2</sup>

1. PhTC LPI RAS, Protvino, Russia  
2. NRC KI – IHEP, Protvino, Russia

Hadron therapy using the pencil beam scanning technique is the most accurate kind of remote radiation therapy. High accuracy is due to the fundamental physical property of protons and ions - to stop in the tissue at a certain depth, the so-called Bragg peak. This is why hadron therapy is used to treat critical organs, in particular the brain. However, accuracy in proton delivery is limited by uncertainty surrounding the hadron beam range. The detector considered in this paper is able to determine the hadron ranges by prompt gamma radiation [3] in real time mode. Basically this detector is planned to use with the proton therapy complex "Prometheus".

**The purpose** of this research was precision statistical simulation of multi-particle radiation transport using a realistic 3D model of clinical setup prototype and the systems of slot-hole collimators for on-line monitoring of Bragg-peak position at a proton therapy complex "Prometheus" to define of an available detecting accuracy and the choice of its optimum parameters. Numerical simulation of the experiments was carried out using the RTS&T [1,2] high-precision radiation transport software package using files of evaluated nuclear data from ENDF/B VII.1 and LA-150 libraries [4].

Fig. 2 illustrates the linear energy deposition and production of prompt  $\gamma$ -rays in inelastic nuclear interactions of primary protons in the water phantom. Definition of Bragg-peak position  $Z_p$  comes down to a problem of longitudinal (along a beam direction) coordinates definition for a spatial point  $Z_\gamma$  in which density of prompt  $\gamma$ -rays production decreases practically to zero:

$Z_p = Z_\gamma - \Delta Z$ , where  $\Delta Z$  - calculated coefficient.

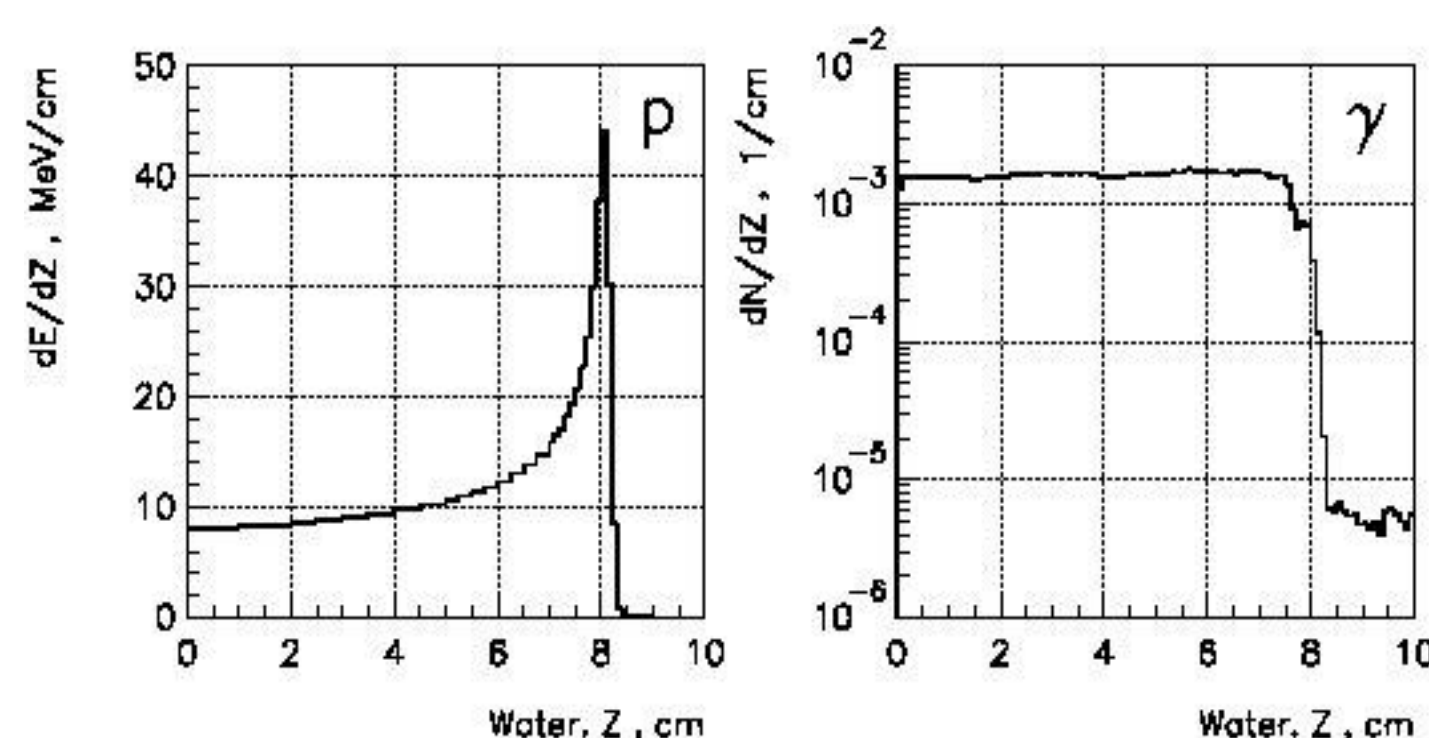


Fig. 2. The deep distribution of energy deposition and the density of prompt  $\gamma$ -rays production from the primary proton beam with an energy of 100 MeV in the water phantom.

The elementary diagram for basic elements of calculated system (the water phantom, collimator system, plate of scintillation detectors) is shown on fig. 3. The prompt  $\gamma$ -rays flux is formed by the system of the slot-hole collimators made of heavy alloys of the residence permit brands (tungsten-nickel-iron, WNiFe). The water phantom is cylinder of 20 cm long and with a radius of 10 cm in which center the proton beam with energy of 100 MeV is dumped. The distance along a beam from a front edge of the collimator to the phantom is 19.2 cm.

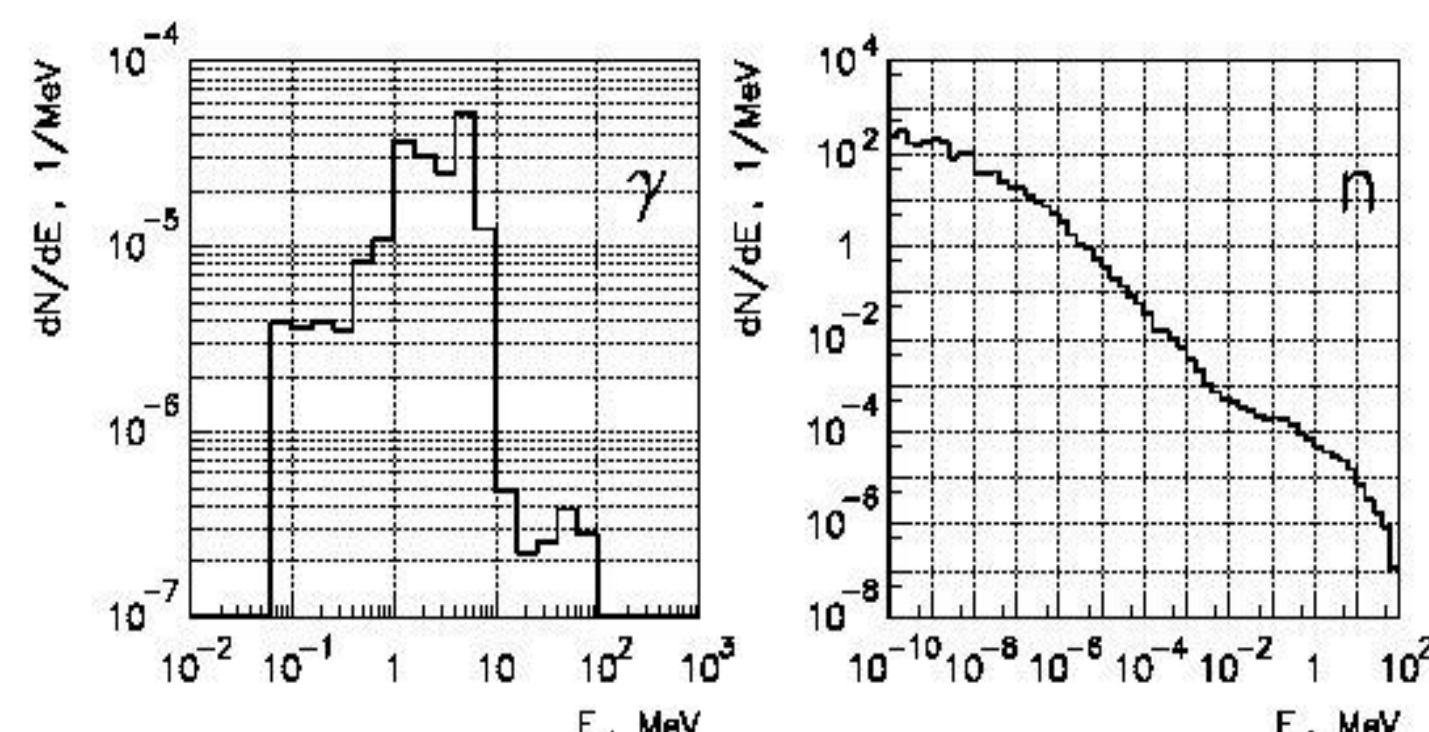


Fig. 5. Energy distributions of prompt  $\gamma$ -rays and neutrons from a primary proton beam with an energy of 100 MeV

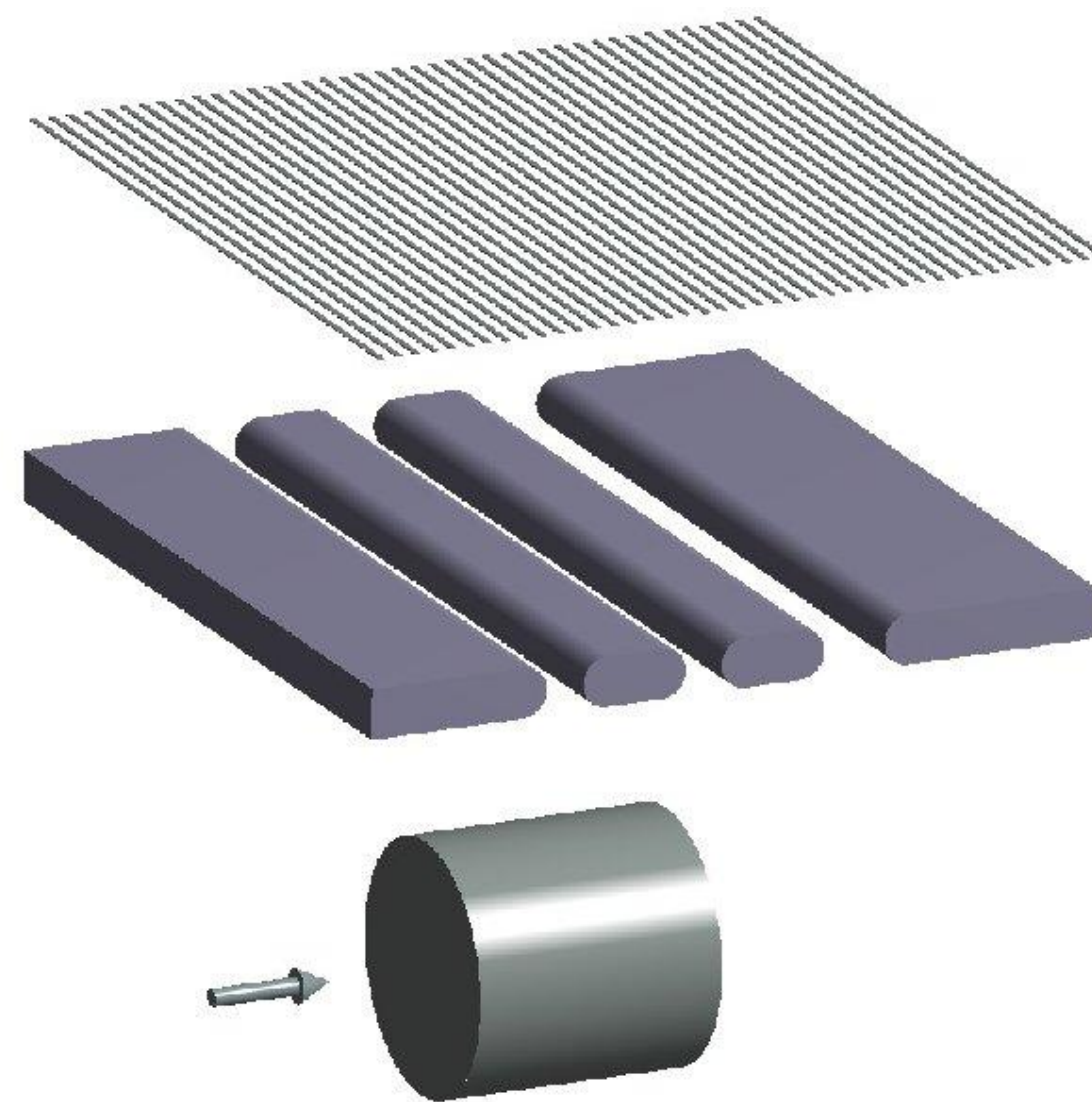


Fig. 3. The design scheme of the clinical setup (general view)

This distance was chosen so that the longitudinal coordinate (8.3 cm) of a point in which the calculated density of prompt  $\gamma$ -rays production in water could already be considered equal to zero (fig. 2) was exactly in the center of the second crack of the collimator ( $19.2 + 8.3 = 27.5$  cm). Apart from 30 to 34 cm from an axis of a beam the collimator 4 cm thick and cross sectional dimensions  $60 \times 60$  cm<sup>2</sup> is located. In the collimator, there are transversal slits with rounded edges. Width of slits along a beam is 3, 3 and 5 cm. The distance along a beam from the beginning of the collimator to the center of slits are 16, 27.5 and 40 cm respectively. At a distance of 60 cm from the beam axis, a  $\gamma$ -rays detector with transverse dimensions also  $60 \times 60$  cm<sup>2</sup> is located strictly above the collimator, showed in Fig. 4.

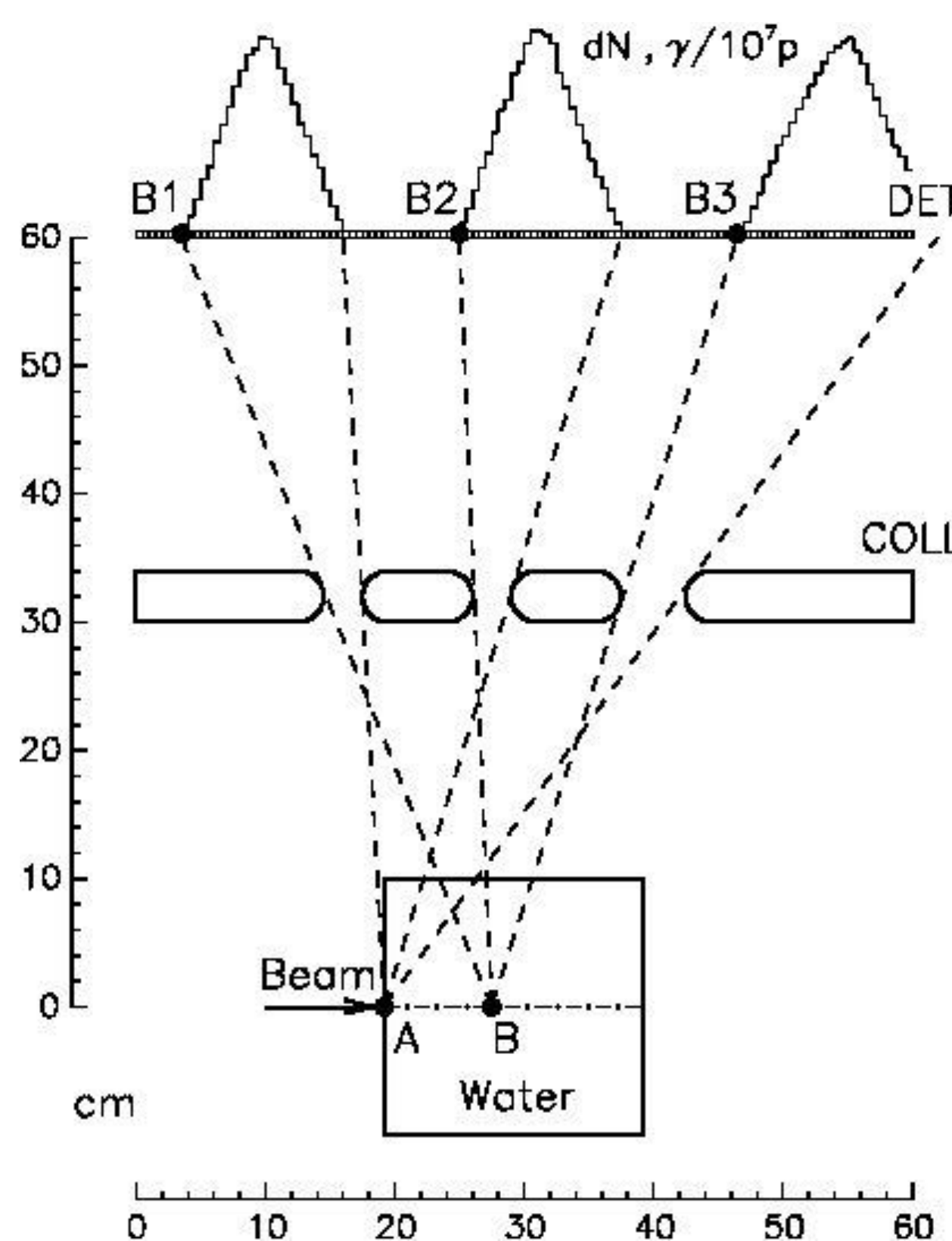


Fig. 4. The design scheme of the clinical setup (side view).

Fig. 4 shows the principle of  $\gamma$ -rays longitudinal coordinate distributions formation on the detector. The upper part of the figure shows of prompt  $\gamma$ -rays distribution in the case of black collimator and without taking into account the neutron background (the distributions presented in Fig. 6). Prompt  $\gamma$ -rays are produced in the water phantom at points whose longitudinal coordinates are in the interval from zero (point A) to 8.3 cm (point B). It can be seen that the lines drawn from the points A and B to the detector and simultaneously tangential to the collimator's cheeks determine three peaks in the detector's distribution in the  $\gamma$ -rays distribution, whose left edges begin at the points B1, B2 and B3, respectively.

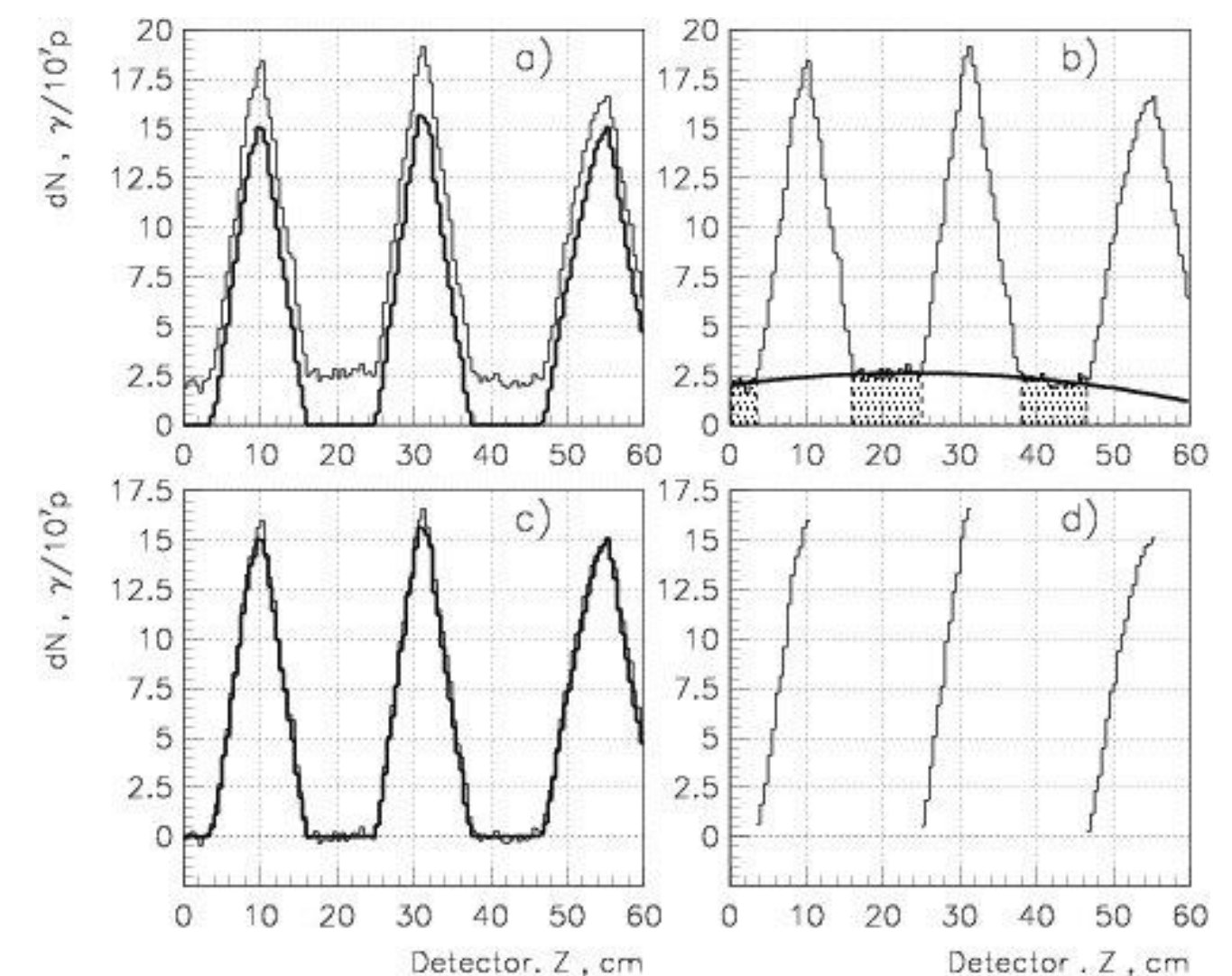


Fig. 6. The distribution along the longitudinal coordinate of prompt  $\gamma$ -rays intensity at the detector. Idealized distribution (thick line) - without taking into account the contribution of neutrons using absolutely black collimators; realistic distribution (thin line) - taking into account the neutron background and realistic WNiFe-collimators): a) - realistic and idealized distribution; b) definition of the background for a realistic distribution; c) realistic without background and idealized distribution. d) the left parts of the peaks of a realistic distribution without background

On fig. 5 the energy distributions for  $\gamma$ -rays and neutrons on the detector plates are presented. Taking into account these distributions (Fig. 7) the optimum type of a scintillator was found - BGO crystal scintillator

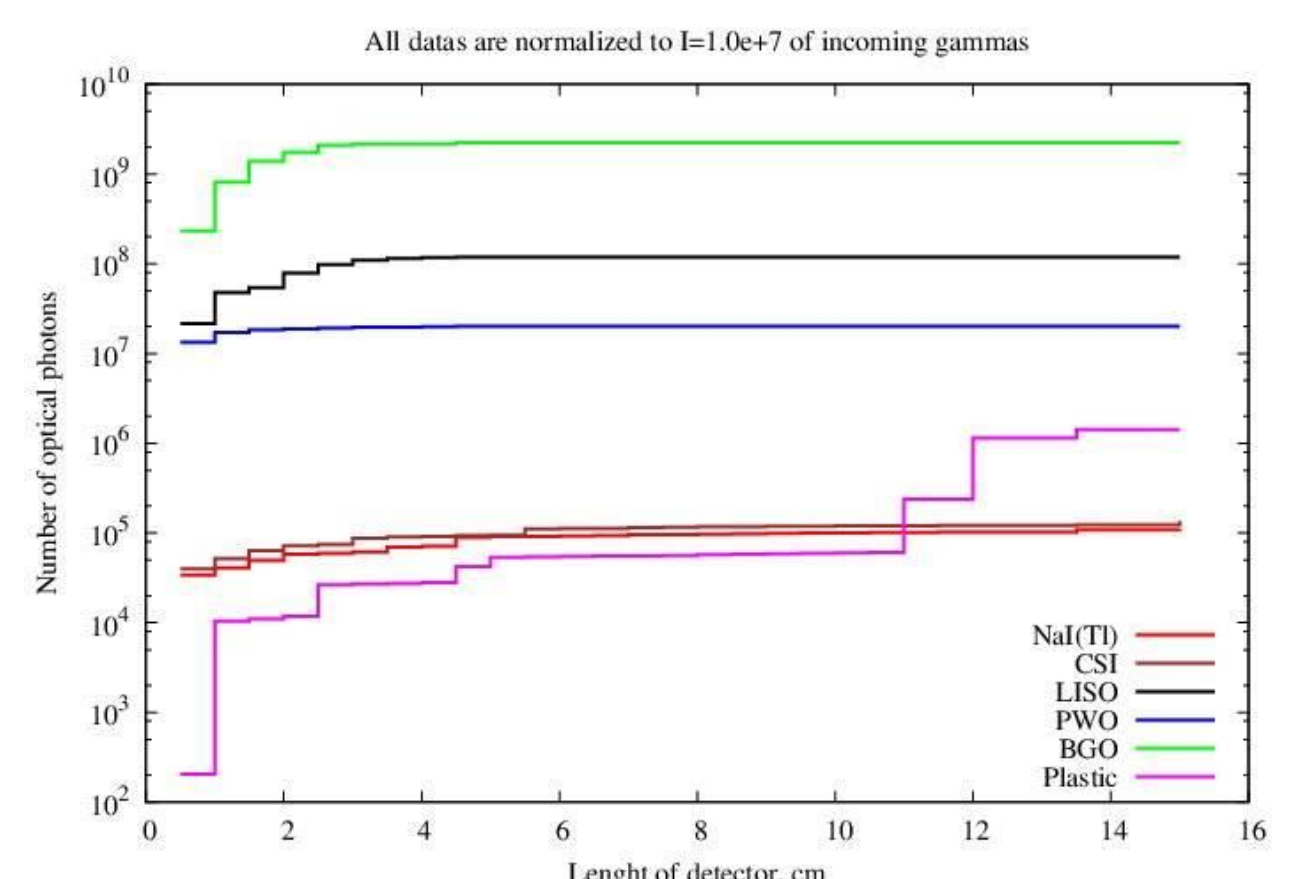


Fig. 7. The light output of the detecting element of the matrix ( $d = 6.0$  mm), made of different types of scintillator.

**Results:** To determine the error of the longitudinal Bragg peak monitoring, a series of 24 calculations was performed using different sequences of pseudo-random numbers to construct trajectories of particles in the calculation system. When using 3 slits, the RMS-error in determining the longitudinal coordinate was 1.5 mm.

## References

- [1] I.I. Degtyarev, F.N. Novoskoltsev, O.A. Liashenko, E.V. Gulina, L.V. Morozova, RTS&T 2014 Code Status, Nuclear Energy and Technology 1(2015) 222-225.
- [2] A.I. Blokhin, I.I. Degtyarev, A.E. Lokhovitskii, M.A. Maslov, and I.A. Yazynin. RTS&T Monte Carlo Code (Facilities and Computation Methods), in.: SARE-3 Workshop, KEK, Tsukuba, Japan, May 1997; INDC (CCP)-426.
- [3] C.-H. Min, C. H. Kim, M.-Y. Youn and J.-W. Kim, Prompt gamma measurements for locating the dose falloff region in the proton therapy, Appl. Phys. Lett., 2006, v. 89, p.183.
- [4] A.A. Pryanichnikov et al., Verification of the world evaluated nuclear data libraries on the basis of integral experiments using the RTS&T code system, Prob. Atom. Sc. and Tec.. Series: Nuclear and Reactor Constants, 1, p. 127, (2018)